



Universiteit  
Leiden  
The Netherlands

## Assessment of functional shunting in patients with sickle cell disease

Afzali-Hashemi, L.; Wood, J.C.; Biemond, B.J.; Nederveen, A.J.; Mutsaerts, H.J.M.M.; Schrantee, A.; Vaclavu, L.

### Citation

Afzali-Hashemi, L., Wood, J. C., Biemond, B. J., Nederveen, A. J., Mutsaerts, H. J. M. M., Schrantee, A., & Vaclavu, L. (2022). Assessment of functional shunting in patients with sickle cell disease. *Haematologica*, 107(11), 2708-2719. doi:10.3324/haematol.2021.280183

Version: Publisher's Version  
License: [Creative Commons CC BY-NC 4.0 license](#)  
Downloaded from: <https://hdl.handle.net/1887/3731433>

**Note:** To cite this publication please use the final published version (if applicable).

# Assessment of functional shunting in patients with sickle cell disease

Liza Afzali-Hashemi,<sup>1</sup> Lena Václavů,<sup>2</sup> John C. Wood,<sup>3</sup> Bart J. Biemond,<sup>4</sup> Aart J. Nederveen,<sup>1</sup> Henk J.M.M. Mutsaerts<sup>1#</sup> and Anouk Schrantee<sup>1#</sup>

<sup>1</sup>Department of Radiology and Nuclear Medicine, Amsterdam University Medical Centers, Amsterdam, the Netherlands; <sup>2</sup>C.J. Gorter Center for High Field MRI, Department of Radiology, Leiden University Medical Center, Leiden, the Netherlands; <sup>3</sup>Division of Cardiology, Children's Hospital Los Angeles, Keck School of Medicine, University of Southern California, Los Angeles, CA, USA and <sup>4</sup>Department of Hematology, Amsterdam University Medical Centers, Amsterdam, the Netherlands

<sup>#</sup>HJMMM and AS contributed equally as co-senior authors.

**Correspondence:** A. Schrantee  
a.g.schrantee@amsterdamumc.nl

**Received:** October 19, 2021.

**Accepted:** May 5, 2022.

**Prepublished:** May 12, 2022.

<https://doi.org/10.3324/haematol.2021.280183>

©2022 Ferrata Storti Foundation

Published under a CC BY-NC license



## Abstract

Silent cerebral infarcts (SCI) are common in patients with sickle cell disease (SCD) and are thought to be caused by a mismatch between oxygen delivery and consumption. Functional cerebrovascular shunting is defined as reduced oxygen offloading due to the rapid transit of blood through the capillaries caused by increased flow and has been suggested as a potential mechanism underlying reduced oxygenation and SCI. We investigated the venous arterial spin labeling signal (VS) in the sagittal sinus as a proxy biomarker of cerebral functional shunting, and its association with hemodynamic imaging and hematological laboratory parameters. We included 28 children and 38 adults with SCD, and ten healthy race-matched adult controls. VS, cerebral blood flow (CBF), velocity in the brain feeding arteries, oxygen extraction fraction (OEF) and cerebral metabolic rate of oxygen (CMRO<sub>2</sub>) were measured before and after acetazolamide administration. VS was higher in patients with SCD compared to controls ( $P < 0.01$ ) and was increased after acetazolamide administration in all groups ( $P < 0.01$ ). VS was primarily predicted by CBF ( $P < 0.01$ ), but CBF-corrected VS was also associated with decreased CMRO<sub>2</sub> ( $P < 0.01$ ). Additionally, higher disease severity defined by low hemoglobin and increased hemolysis was associated with higher CBF-corrected VS. Finally, CMRO<sub>2</sub> was negatively correlated with fetal hemoglobin, and positively correlated with lactate dehydrogenase, which could be explained by changes in oxygen affinity. These findings provide evidence for cerebral functional shunting and encourage future studies investigating the potential link to aberrant capillary exchange in SCD.

## Introduction

Sickle cell disease (SCD) is characterized by chronic hemolytic anemia resulting in organ damage including silent cerebral infarcts (SCI).<sup>1,2</sup> SCI are associated with cognitive impairment at an early stage in life, which can result in under- and unemployment as well as lower quality of life.<sup>2,3</sup> SCI are primarily localized in deep white matter and are hypothesized to be a result of impaired oxygen delivery.<sup>4-6</sup> In order to maintain brain oxygenation, cerebral blood flow (CBF) is increased in patients with SCD.<sup>7-9</sup> However, despite the preservation of normal global oxygen delivery at rest,<sup>10</sup> the incidence of SCI continues to rise throughout the lifetime of these patients and is prevalent in more than 50% of adult SCD patients by the age of 32 years.<sup>11</sup> One potential pathophysiological mechanism that has been proposed suggests that SCI result from localized

impairments in oxygen delivery caused by cerebral functional shunting.<sup>10,12,13</sup> Cerebral functional shunting is defined as the rapid transit of blood through the brain capillaries as a result of increased flow, limiting offloading of oxygen to the tissue.<sup>13</sup> However, functional shunting is difficult to assess and more insight into this process is required to understand the underlying cerebral hemodynamics in SCD.

Arterial spin labeling (ASL) magnetic resonance imaging (MRI) is widely used in research settings as a non-invasive technique for cerebral perfusion measurements in patients with SCD.<sup>9,14,15</sup> ASL applies radiofrequency pulses in the brain feeding arteries that change the magnetization of blood, also known as labeling. Following labeling, the blood travels to the brain and a labeled image is acquired. The same procedure is repeated without labeling to acquire a control image. By subtracting the labeled image

from the control image, a quantitative perfusion map is obtained. A requirement of ASL is that images are acquired after a predefined delay (post-label delay), allowing the labeled blood to travel to the capillary bed, and for the labeled spins to enter the tissue. The difference between labeled spins detected in arterial and venous circulations represents spins that have exchanged with the brain parenchyma.<sup>16</sup> According to the Renkin-Crone model, which relates blood flow to extraction fraction, the amount of unexchanged labeled spins in the venous outflow, i.e., the venous signal (VS), will increase approximately proportionally with CBF.<sup>17,18</sup> However, in the presence of cerebral functional shunting, a larger volume of the labeled blood will pass unexchanged through the capillaries and may arrive on the venous side at the time of imaging. Indeed, a previous study demonstrated that, with longer post-label delays, the VS in the sagittal sinus can be used to inform on the exchange of spins at the capillary level.<sup>16</sup> As such, VS may provide additional hemodynamic information about oxygen utilization at the capillary level, which may be affected in patients with SCD.

Support for this hypothesis comes from prior work in SCD patients.<sup>13,19,20</sup> Juttukonda et al.<sup>13,20</sup> observed the presence of ASL signal in the venous sinuses at a regular post-label delay (1,900 ms), which was associated with increased CBF and elevated velocities in the carotid arteries. When administered to adult patients with SCD, acetazolamide (ACZ; a compound that induces vasodilation and increased CBF) led to observed reductions in oxygen extraction fraction (OEF) as well as the cerebral metabolic rate of oxygen (CMRO<sub>2</sub>),<sup>10</sup> indicating that oxygen consumption can actually deteriorate despite increasing oxygen delivery. Moreover, in SCD patients with SCI, an inverse relation between VS scores and OEF was found, providing support for a mechanism involving functional shunting.<sup>20</sup> However, whether VS relates to cerebral functional shunting and could therefore be a marker of capillary oxygen exchange efficiency in SCD patients, remains to be investigated.

Therefore, in the present study, we investigated cerebral functional shunting in patients with SCD, by examining the relationship between VS and cerebrovascular imaging parameters of perfusion, cerebral oxygen extraction and metabolism as well as laboratory measures. In order to directly probe the VS-CBF relationship, we studied the imaging parameters both before and after ACZ administration in adult participants.

## Methods

The data were obtained from two studies<sup>6,21</sup> (one adult and one pediatric study) that were approved by the medical ethics committee of Academic Medical Center in Amster-

dam and performed in accordance with the Declaration of Helsinki. Written informed consent was obtained from all adults and from parents/legal guardians of participants in the pediatric study cohort. Sixty-six patients with SCD (59 HbSS and 7 HbSβ<sup>0</sup>thalassemia) were recruited from hematology outpatient clinics.<sup>6,21</sup> Additionally, ten healthy adult race-matched controls (8 HbAA and 2 HbAS) were recruited. Exclusion criteria were MRI contraindications, history of cerebral pathology, sickle cell crisis at inclusion, hospitalization 1 month prior to the study day, pregnancy, and ACZ contraindications for adult participants.

### Data acquisition

Images were acquired on two 3.0 T MRI systems (Philips Intera and Ingenia, Philips Healthcare, Best, the Netherlands) with an 8-channel head coil for pediatric patients and a 32-channel head coil for adults. Prior to MRI, blood was drawn to quantify hematological laboratory parameters (for details, see the *Online Supplementary Appendix*). Anatomical sequences included a 2D T<sub>2</sub>-weighted and a 2D fluid-attenuated inversion recovery (FLAIR) scan for children and 3D FLAIR for adult participants were used for lesion and gray matter segmentation, and registration purposes.

For VS and CBF measurements, pseudo-continuous arterial spin labeling (pCASL) was used (Table 1). Adult participants received intravenous ACZ (16 mg/kg with a maximum of 1,400 mg) 10 minutes prior to the second ASL scan.

In order to obtain venous saturation for OEF measurements in adult participants' pre- and post-ACZ, T<sub>2</sub>-prepared tissue Relaxation with an Inversion Recovery MRI (T<sub>2</sub>-TRIR) sequence<sup>22</sup> was used. Finally, to obtain velocity measurements in the brain feeding arteries, a 2D phase-contrast single-shot gradient-echo T<sub>1</sub> FFE sequence was acquired both pre- and post-ACZ (Table 1) (for more details on the acquisition parameters, see the *Online Supplementary Appendix*).

### Data analysis

VS was assessed both qualitatively and quantitatively. Qualitatively, ASL images were visually inspected by an observer (LA) for the presence or absence of the venous ASL signal. Quantitatively, we scaled the perfusion-weighted signal (control-label) from the ASL images, by the group-based T<sub>1</sub> of blood (patients = 1,818 ms<sup>23</sup> and controls = 1,650 ms<sup>24</sup>), subject-specific estimates of labeling efficiency based on velocity,<sup>25</sup> and M0 in ExploreASL.<sup>26</sup> The superior sagittal sinus and straight sinus were manually segmented in three group-average (children and adults with SCD and healthy control group) images of all participants in standard MNI space<sup>27</sup> (Figure 1). The segmented average image of each group was resampled to the native ASL space of each individual and used as an

**Table 1.** Scan parameters of functional scans in children and adult subjects.

	pCASL		Phase contrast		T <sub>2</sub> -TRIR
	children	adults	children	adults	adults
TR, ms	4,000	4,400	15	15	150
TE, ms	17	14	5	6	24
Flip angle,°	90	90	15	15	95
2D / 3D	2D	2D	2D	2D	2D
FOV, mm	240x240x119	240x240x133	230x230x4	230x230x4	202x243x4
Voxel size, mm	3x3x7	3x3x7	0.45x0.45x4	0.45x0.45x4	2x2x4
PLD, ms	1,525	1,800	-	-	-
Label duration, ms	1,650	1,800	-	-	-
VENC, cm/s	-	-	140	80	-
Scan duration, mm:ss	10:12	5:00	1:05	1:05	0:50

pCASL: pseudo-continuous arterial spin labeling; T<sub>2</sub>-TRIR: T<sub>2</sub>-prepared tissue relaxation with an inversion recovery; TR: repetition time; TE: echo time; FOV: field of view; PLD: post-label delay, VENC: velocity encoding.

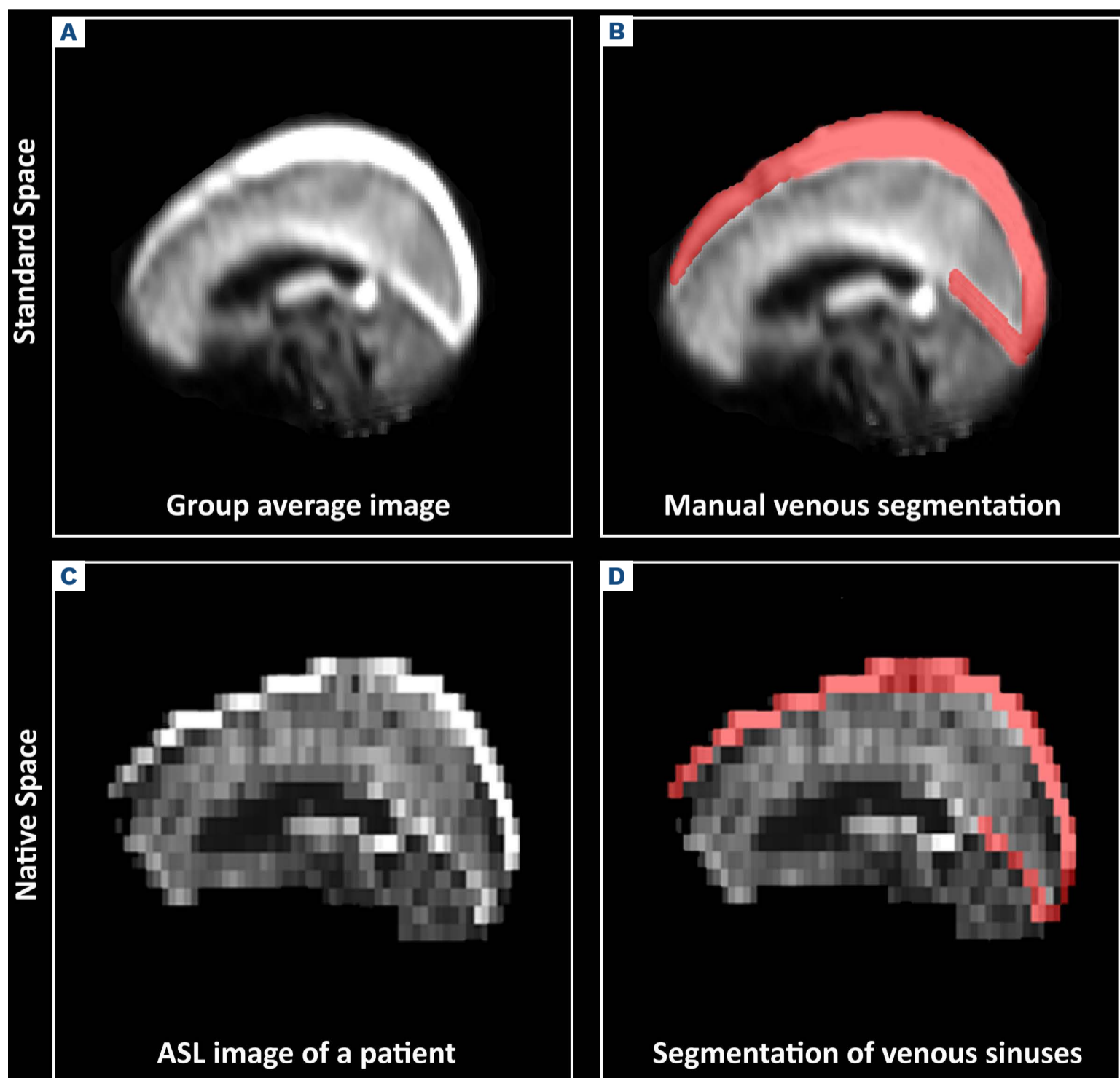


**Figure 1.** An example of the semi-automatic segmentation method of the sagittal and straight sinuses. (A) Sagittal group-average image in standard space. (B) Manual segmentation of the venous signal (VS) in image (A). (C) Image in native arterial spin labeling (ASL) space of a representative patient. (D) Red overlay of the segmented VS on the ASL image.

ASL mask from which the average VS is measured. In case the segmented venous sinuses were not correctly aligned after resampling, manual correction was applied to only include the VS. In addition, subject-specific gray matter masks were used in the native space to measure the mean signal in the GM. For the comparison between children and adults, the proportion of signal in the venous regions of interest (ROI) relative to GM was calculated in the VS images (VS/GM). This ratio is referred to as VGR henceforth. Taking the ratio rather than VS cancels out global physiological perfusion confounders and imaging

acquisition differences and allows a comparison between the pediatric and adult group. However, the VS was used to study the associations between VS and other hemodynamic parameters within each group.

CBF, OEF and  $CMRO_2$  were calculated as described in the previous studies<sup>10,21</sup> and are illustrated in Figure 2 and described in the *Online Supplementary Appendix*, together with the analysis of the velocity in the brain feeding arteries. White matter lesions were delineated on FLAIR images using manual segmentation and quantified as previously described.<sup>6,21</sup>

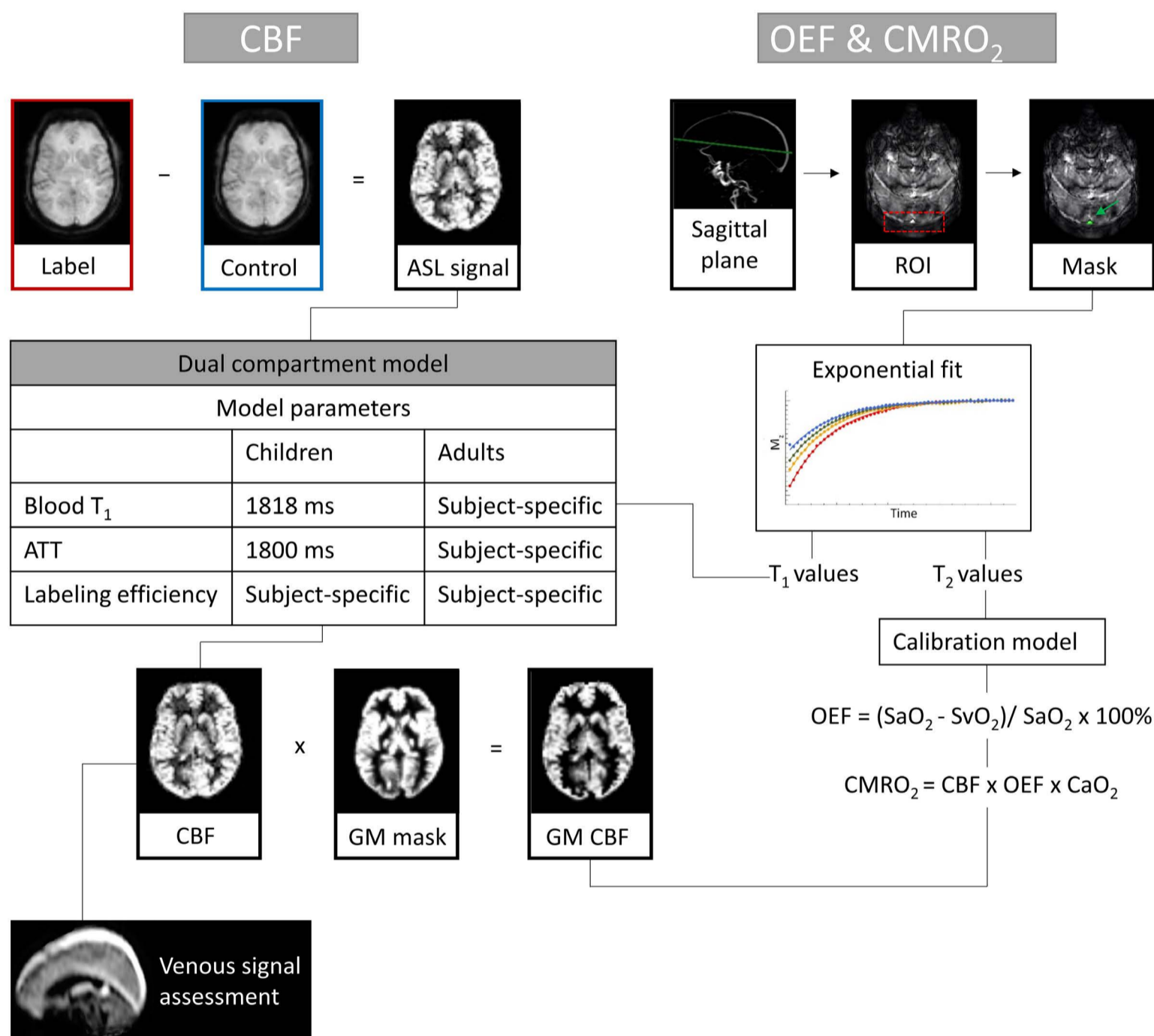


**Figure 2. Visual representation of the image analysis steps.** Left: the arterial spin labeling (ASL) signal was obtained by subtracting the control images from the labeled images. Cerebral blood flow (CBF) was then quantified using the dual compartment model and the obtained CBF image was multiplied by the gray matter (GM) mask (created from anatomical images not shown here) to obtain the GM CBF image. CBF images were also used for venous signal assessment. Right:  $T_2$ -prepared tissue relaxation with an inversion recovery magnetic resonance imaging ( $T_2$ -TRIR) images were used to obtain the  $T_1$  and  $T_2$  values of venous blood. An automatic localizer tool was used to detect the region of interest in the posterior part of the brain (in red). This tool searched for high-intensity signals in the last 7 phases of the magnitude reconstructed  $T_2$ -TRIR data to detect the sagittal sinus. Subsequently, a fit was initiated in the sagittal sinus voxels (shown in green on the mask image). The fitted  $T_1$  values were used for CBF quantification in adults and the fitted  $T_2$  values were converted to venous oxygen saturation using the hemoglobin A (HbA) and HbS calibration models. Subsequently, the venous oxygen saturation and arterial oxygen saturation (assumed to be 0.98) were used to calculate the oxygen extraction fraction (OEF).  $CMRO_2$  was obtained by multiplying the OEF by the CBF and oxygen-carrying capacity ( $CaO_2$ ). For details, see the *Online Supplementary Appendix*. ATT: arterial transit time.

### Statistical analyses

Statistical analyses were performed in SPSS v26 (IBM, NY, USA).  $P < 0.05$  was considered statistically significant. Independent  $t$ -tests and paired-sample  $t$ -tests (or non-parametric alternatives in case of non-normality) were performed to test differences between the groups and to test the statistical differences of VGR before and after ACZ administration. We performed the correlation analysis to assess the relationship between VS and CBF. In order to test if VS contained additional hemodynamic information independently from CBF, the residuals of the regression between VS and CBF ( $VS_{CBF}$ ) were used as the dependent variable in stepwise multiple linear regression analyses against age, sex, participant groups, hydroxy-

urea, hemoglobin (Hb; as a measure of anemia) and lactate dehydrogenase (LDH) (as a measure of hemolysis) for the baseline data. In order to test the role of oxygen metabolism and ACZ on VS in adult participants, linear mixed-effects modeling was performed, in which OEF,  $CMRO_2$  and ACZ condition were added as additional predictors.

In order to further explore the relationship between parameters of oxygen metabolism and hemodynamic and laboratory parameters in adult SCD patients, we performed linear mixed-effects modeling with  $CMRO_2$ , corrected for  $VS_{CBF}$  as the dependent variable. The predictors tested in the model were CBF, VS, Hb, LDH, HbF, and ACZ condition.

**Table 2.** Demographic, clinical and imaging summary of participants.

	Pediatric SCD	Adult SCD	Controls	P-value	
	N=28	N=38	N=10	PSCD vs. ASCD	ASCD vs. CTL
<b>Demographics</b>					
Age in years, mean $\pm$ SD	12.7 $\pm$ 2.3	32.1 $\pm$ 11.2	36.4 $\pm$ 15.9	< 0.01	0.74
Female, N (%)	9 (32%)	14 (37%)	4 (40%)	0.69	0.85
<b>Clinical parameters</b>					
Hemoglobin, gr/dL, mean $\pm$ SD	8.4 $\pm$ 1.1	8.8 $\pm$ 1.4	13.9 $\pm$ 1.2	0.14	< 0.01
Hematocrit, %, mean $\pm$ SD	23 $\pm$ 3	26 $\pm$ 4	42 $\pm$ 3	< 0.01	< 0.01
Reticulocytes $\times 10^9/L$ , mean $\pm$ SD	277.7 $\pm$ 106.7	260.2 $\pm$ 108.2	63.1 $\pm$ 24.4	0.60	< 0.01
LDH, U/L 37°C, mean $\pm$ SD	514 $\pm$ 110	460 $\pm$ 160	181 $\pm$ 41	0.12	< 0.01
Total Bilirubin, mg/dL, mean $\pm$ SD	3.5 $\pm$ 2.2	3.5 $\pm$ 2.8	0.7 $\pm$ 0.48	0.85	< 0.01
HbF, %, mean $\pm$ SD	9.8 $\pm$ 5.1	9.1 $\pm$ 7.6	-	0.20	-
HbS, %, $\pm$ DS	85.8 $\pm$ 4.6	80.4 $\pm$ 15.1	37.0 $\pm$ 0.4	0.52	0.02
Hydroxyurea, N of patients (%)	9 (32%)	15 (39%)	-	0.44	-
Ex transfusions N of patients (%)	-	3 (8%)	-	-	-
<b>Imaging parameters</b>					
CBF <sub>GM</sub> , mL/100 gr/min, mean $\pm$ SD					
pre-ACZ	96.8 $\pm$ 14.7	85.8 $\pm$ 15.4	52.7 $\pm$ 3.15	< 0.01	< 0.01
post-ACZ	-	113.3 $\pm$ 22.0	88.9 $\pm$ 9.9	-	< 0.01
VGR, mean $\pm$ SD					
pre-ACZ	2.4 $\pm$ 0.8	2.0 $\pm$ 0.9	0.6 $\pm$ 0.5	0.08	< 0.01
post-ACZ	-	2.8 $\pm$ 0.7	2.0 $\pm$ 0.6	-	< 0.01
Weighted velocity, cm/s, mean $\pm$ SD					
pre-ACZ	27.5 $\pm$ 5.3	24.5 $\pm$ 4.7	17.5 $\pm$ 2.6	0.03	< 0.01
post-ACZ	-	30.7 $\pm$ 5.0	24.2 $\pm$ 4.9	-	< 0.01
OEF, %, mean $\pm$ SD					
pre-ACZ	-	27.2 $\pm$ 4.4	35.4 $\pm$ 3.4	-	< 0.01
post-ACZ	-	19.0 $\pm$ 5.8	20.1 $\pm$ 7.6	-	0.64
$CMRO_2$ , $\mu$ mol O <sub>2</sub> /100 g/min, mean $\pm$ SD					
pre-ACZ	-	99.8 $\pm$ 24.2	128.6 $\pm$ 20.3	-	< 0.01
post-ACZ	-	90.7 $\pm$ 28.6	127.5 $\pm$ 46.0	-	0.01
Lesion volume, mL, mean $\pm$ SD	1.3 $\pm$ 4.1	3.9 $\pm$ 8.1	0.2 $\pm$ 0.3	< 0.01	0.03
Lesion presence, N (%)	17 (61%)	31 (82%)	8 (80%)	0.06	0.91

$P$ -values were calculated using independent-sample  $t$ -tests or Mann-Whitney test in case of non-normality, or Pearson's Chi-square test for categorical variables. PSCD: pediatric sickle cell disease (SCD); ASCD: adult SCD; CTL: control; F: female; LDH: lactate dehydrogenase; Hb: hemoglobin; CBF: cerebral blood flow; GM: gray matter; ACZ: acetazolamide; VS: venous signal; VGR: VS to gray matter signal ratio; OEF: oxygen extraction fraction;  $CMRO_2$ : cerebral metabolic rate of oxygen.

## Results

Demographic, clinical and imaging parameters of 28 pediatric patients with SCD, 38 adult patients and ten healthy controls are presented in Table 2. The *Online Supplementary Table S1* shows the available sample size for each included parameter. Of this sample, nine (32%) pediatric and 15 (39%) adult patients were using hydroxyurea. In the adult SCD group, three (8%) patients received regular blood exchange transfusions and were studied 3-28 days since their last transfusion.

### Venous arterial spin labeling signal

Venous ASL signal was observed in 27 (96%) pediatric patients, 36 (95%) adult patients and one (10%) healthy control. After ACZ administration, VS was observed in all adult participants (Figure 3A). VGR was significantly higher in patients compared to controls ( $Z=-4.24$ ,  $P<0.01$ ), but not between pediatric and adult SCD patients ( $t=-1.78$ ,  $P=0.08$ ) (Figure 3B). After ACZ administration, VGR increased in adult patients ( $t=-6.10$ ,  $P<0.01$ ) and controls ( $Z=2.80$ ,  $P<0.01$ ) compared to baseline VGR (Figure 3B). No significant VGR differences were found between patients receiving hydroxyurea and those not receiving this intervention.

### Associations of venous signal with other parameters

We observed a positive relationship between baseline CBF and baseline VS ( $R^2=0.59$ ;  $F(1,73)=104.4$ ,  $P<0.001$ ; Figure 4A). After ACZ administration, these associations remained significant ( $R^2=0.57$ ;  $F(1,45)=59.4$ ,  $P<0.001$ ; Figure 4B). No significant association was found between VS and lesion volume in patients with SCD ( $\beta=-0.002$ ,  $P=0.89$ ). Sub-

sequently, we tested associations with baseline  $VS_{CBF}$  in all participants. Stepwise multiple regression analysis demonstrated significant associations with Hb ( $\beta=-0.26$ ,  $P<0.001$ ) and participant group ( $\beta=0.55$ ,  $P=0.004$ ; total model  $R^2=0.23$ ). Subsequent analyses demonstrated a negative correlation between Hb and  $VS_{CBF}$  in the combined patient groups ( $\beta=-0.45$ ,  $P<0.001$ ), but not in the control group ( $\beta=0.02$ ,  $P=0.85$ ) (Figure 5A). After splitting the patient groups, the association between Hb and  $VS_{CBF}$  remained significant in both adults ( $\beta=-0.43$ ,  $P<0.001$ ) and children ( $\beta=-0.45$ ,  $P=0.02$ ) with SCD.

For adult participants, we added OEF,  $CMRO_2$  and ACZ condition as additional parameters and used a linear mixed model to accommodate the repeated measures dependencies. The strongest predictor of  $VS_{CBF}$  was  $CMRO_2$  ( $\beta=-0.79$ ,  $F(1,81)=-24.5$ ,  $P<0.001$ ), demonstrating that subjects with lower  $CMRO_2$  showed higher VS, independent of CBF (Figure 5B). Subsequently, participant group (adult SCD vs. controls) in combination with either Hb (model 1) or LDH (model 2) were significant additional predictors (model 1:  $CMRO_2$   $\beta=-0.75$ ,  $F(1,82)=19.8$ ,  $P<0.001$  / group  $\beta=-69.6$ ,  $F(1,72)=11.5$ ,  $P=0.001$  / Hb  $\beta=-11.6$ ,  $F(1,78)=11.7$ ,  $P=0.001$ ; model 2:  $CMRO_2$   $\beta=-0.92$ ,  $F(1,78)=27.8$ ,  $P<0.001$  / group  $\beta=-40.1$ ,  $F(1,78)=5.4$ ,  $P=0.023$  / LDH  $\beta=0.11$ ,  $F(1,79)=10.0$ ,  $P=0.002$ ). When splitting the group into SCD adults and controls, we observed that in addition to  $CMRO_2$ , Hb and LDH were significant independent predictors of  $VS_{CBF}$  in patients (but not in controls) with Hb being a negative predictor ( $\beta=-14.2$ ,  $P<0.001$ ) and LDH being a positive predictor ( $\beta=0.13$ ,  $P=0.002$ ). We repeated our statistical analyses excluding the three patients receiving exchange transfusion and found comparable results.

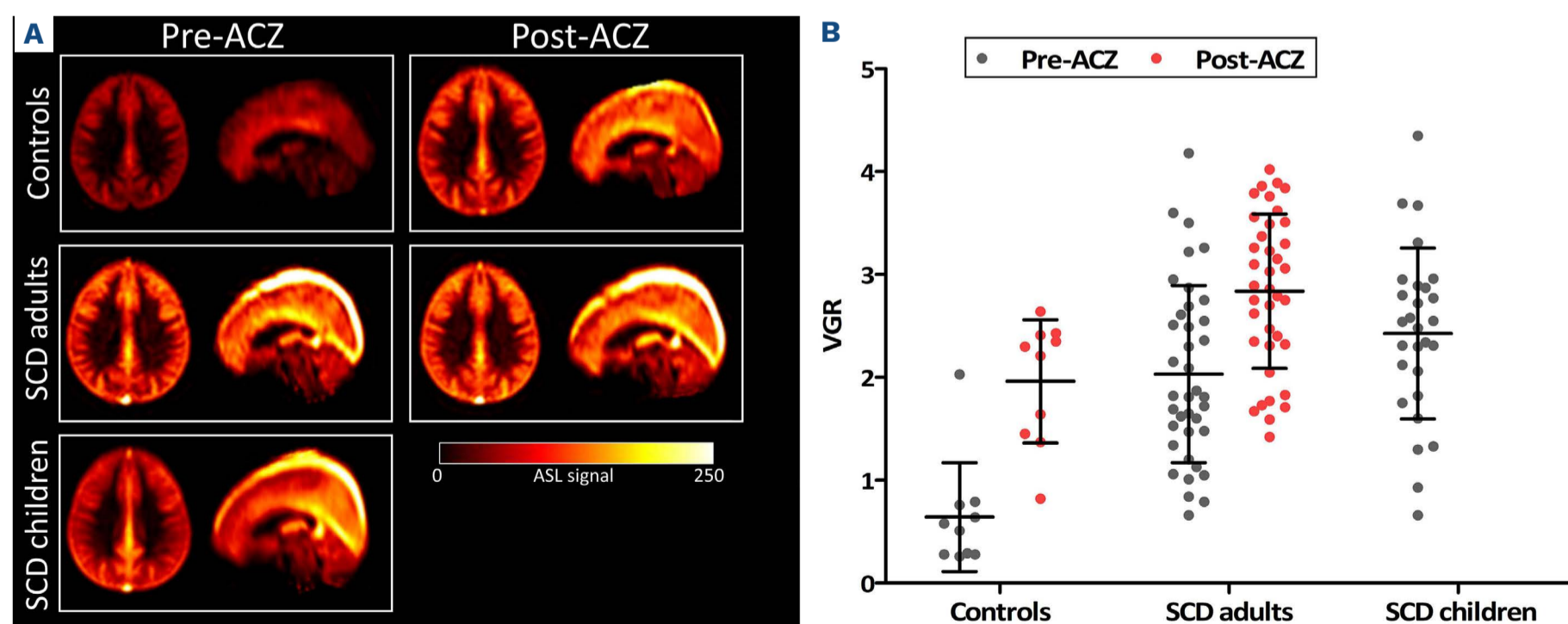


**Figure 3. Venous signal across groups.** (A) Group average axial and sagittal arterial spin labeling (ASL) images in Montreal Neurological Institute (MNI) space before and after acetazolamide (ACZ) administration. In healthy controls, venous signal (VS) is minimal at baseline (pre-ACZ) but appears after ACZ administration. (B) Dot plots and the mean with the standard deviation of VS to gray matter signal ratio (VGR) between the groups.

In order to assess further contributing factors to  $CMRO_2$  in SCD patients, we explored the relationships between  $CMRO_2$  and the various hemodynamic and hematological markers. Linear mixed modeling demonstrated that HbF and LDH were significant predictors of  $CMRO_2$  when corrected for  $VS_{CBF}$ . Higher HbF was associated with lower  $CMRO_2$  ( $\beta=-1.4$ ,  $F(1,56)=23.4$ ,  $P<0.001$ ) and higher LDH was associated with higher  $CMRO_2$  ( $\beta=0.05$ ,  $F(1,61)=8.5$ ,  $P=0.005$ ). As HbF is increased by hydroxyurea, we further split the data into hydroxyurea and no hydroxyurea groups to investigate its effects. The associations between HbF and  $CMRO_2$ , and LDH and  $CMRO_2$  were similar across both groups.

## Discussion

The purpose of this study was to investigate cerebral functional shunting in patients with SCD, by means of exploring the relationship between the VS intensity in ASL images and cerebral circulation and oxygen metabolism. Our results confirmed prior observations of higher VS in patients with SCD compared to healthy controls, although no differences between pediatric and adult patients were observed. Our VS data showed a strong association with CBF, confirming that venous outflow is indeed strongly dependent on the inflow to the brain. A key finding of this study was that the CBF-corrected VS was negatively associated with  $CMRO_2$ , demonstrating that VS contains important information about microvascular oxygen offloading, providing evidence for functional shunting. Additionally, higher disease severity, as reflected by more severe anemia and hemolysis was, independently of CBF, associated with higher VS. Finally, in addition to potential cerebral shunting mechanisms in SCD patients, we found that  $CMRO_2$  was further negatively correlated with HbF

and positively correlated with LDH.

The oxygen-carrying capacity of blood in patients with SCD is reduced and as a result, compensatory increases of CBF are observed.<sup>7-9</sup> Previous studies using both continuous and categorical estimates of  $VS^{13,28,29}$  observed that higher perfusion in SCD patients results in the presence of venous ASL signal at standard post-label delays, and the results of the current study corroborate these findings. In addition to CBF, microvascular permeability affects the fraction of labels arriving in the venous sinuses. In case of endothelial dysfunction, the permeability-surface area product (PS), defined as the flow of molecules through the capillary membranes in a certain volume of tissue, may be altered. At physiologically plausible CBF levels and in subjects with intact microvasculature, labeled spins enter the tissue and barely any VS is observed (Figure 6A). In case of increased CBF (e.g., after ACZ administration) and intact PS, VS can be observed in the brain (Figure 6B). However, at elevated CBF with low PS, we expect more labeled spins to pass unexchanged into the cerebral venous circulation (Figure 6C), a process we refer to as microvascular shunting. Importantly, our current findings provide empirical evidence for shunting, by showing that higher VS (independently of CBF) is associated with lower  $CMRO_2$ . Our results are concordant with decreased OEF values observed in SCD patients with categorically increased venous signal scores.<sup>20</sup> Taken together, these data suggest that the venous signal, beyond that expected for a given CBF, is a biomarker of cerebral functional shunting, which might be a result of PS reduction.

The inverse relation between CBF and the parameters OEF and  $CMRO_2$  in chronic anemia might seem paradoxical, but can be explained by physiological mechanisms at the capillary level. Low Hb levels trigger reciprocal increases in CBF to preserve resting oxygen delivery. However, elevated

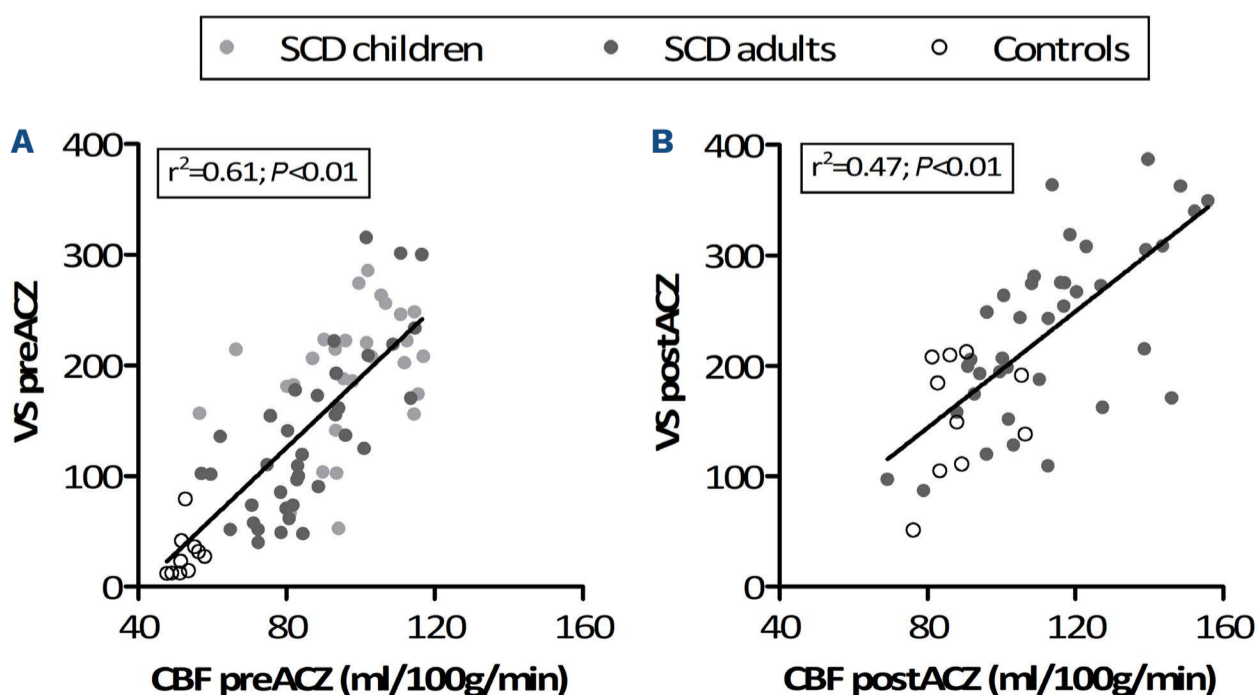


**Figure 4. Association between venous signal and cerebral blood flow.** Scatterplots of mass associations between venous signal (VS) and gray matter cerebral blood flow (CBF) before (left) and after (right) acetazolamide (ACZ). SCD: sickle cell disease administration.



CBF results in decreased capillary transit times, potentially promoting trans-capillary pressure, and increasing heterogeneity in transit times across capillaries in the vascular bed.<sup>30,31</sup> As oxygen extraction is dependent on the time the blood resides in the capillary network, elevated CBF can result in lower OEF and  $CMRO_2$ . However, it is important to consider our findings with respect to the existing body of literature. Studies using  $T_2$ -relaxation-under-spin-tagging (TRUST) have shown increased, unaffected or decreased OEF values in patients with SCD compared to controls,<sup>13,19,20,32,33</sup> depending on the calibration model used for the SCD patients. Inconsistent OEF values were also found using other techniques, with a previous PET study showing no differences in OEF and  $CMRO_2$  between patients and controls,<sup>7</sup> whereas studies applying susceptibility MRI techniques reported both increased or decreased OEF values in SCD patients.<sup>34–36</sup> Our findings cannot be fully attributed to microvascular shunting per se, as we did not assess shunting locally at the capillary level, but rather used VS as a proxy. Nevertheless, although anatomical shunts in this population have been reported,<sup>37,38</sup> microvascular shunting seems the most likely explanation, given the relation between VS and  $CMRO_2$  in the current study, and a previous report showing a reduction of VS after blood transfusion.<sup>39</sup> Interestingly, a very recent study using multi-TI ASL showed that despite lower bolus arrival times in the tissue, much longer arrival times were found in the sagittal sinus of patients with SCD compared to controls, suggesting that hyperperfusion in the arterial tree may be accompanied by al-

tered capillary and/or venular micro-circulatory flow patterns, potentially due to microvascular resistance.<sup>29</sup> Future studies are needed to further elucidate these processes in SCD at the capillary level.

Increased VS beyond that expected for a given CBF ( $VS_{CBF}$ ) might represent a reduction in PS that may be pathological. We demonstrated an inverse relationship of  $VS_{CBF}$  with Hb in both pediatric and adult patients. In adults,  $VS_{CBF}$  was also highly correlated with LDH. This may indicate that SCD patients with higher disease severity, i.e., more anemia and hemolysis, have lower functional cerebral microvascular surface area. Further studies are needed to confirm this hypothesis and to investigate if such changes represent permanent damage or a reversible physiologic phenotype.

We demonstrated that besides VS,  $CMRO_2$  was also influenced by HbF and LDH. Whereas HbF reduces HbS polymerization, which diminishes the complications of SCD, we found a negative association of HbF with  $CMRO_2$ . This negative association is likely a result of the higher oxygen-binding affinity of HbF compared to HbA,<sup>40</sup> potentially resulting in lower oxygen extraction and  $CMRO_2$  for the same CBF. Notably, the HbF effect was not driven specifically by patients on hydroxyurea. The positive association between LDH and  $CMRO_2$  most likely reflects the impact of dense red blood cells (DRBC) on the Hb-dissociation curve. DRBC are an important biomarker of SCD severity because of their predisposition for polymerization and hemolysis. Dense cells have markedly low oxygen affinity<sup>41</sup> which would facilitate oxygen extraction. Indeed,

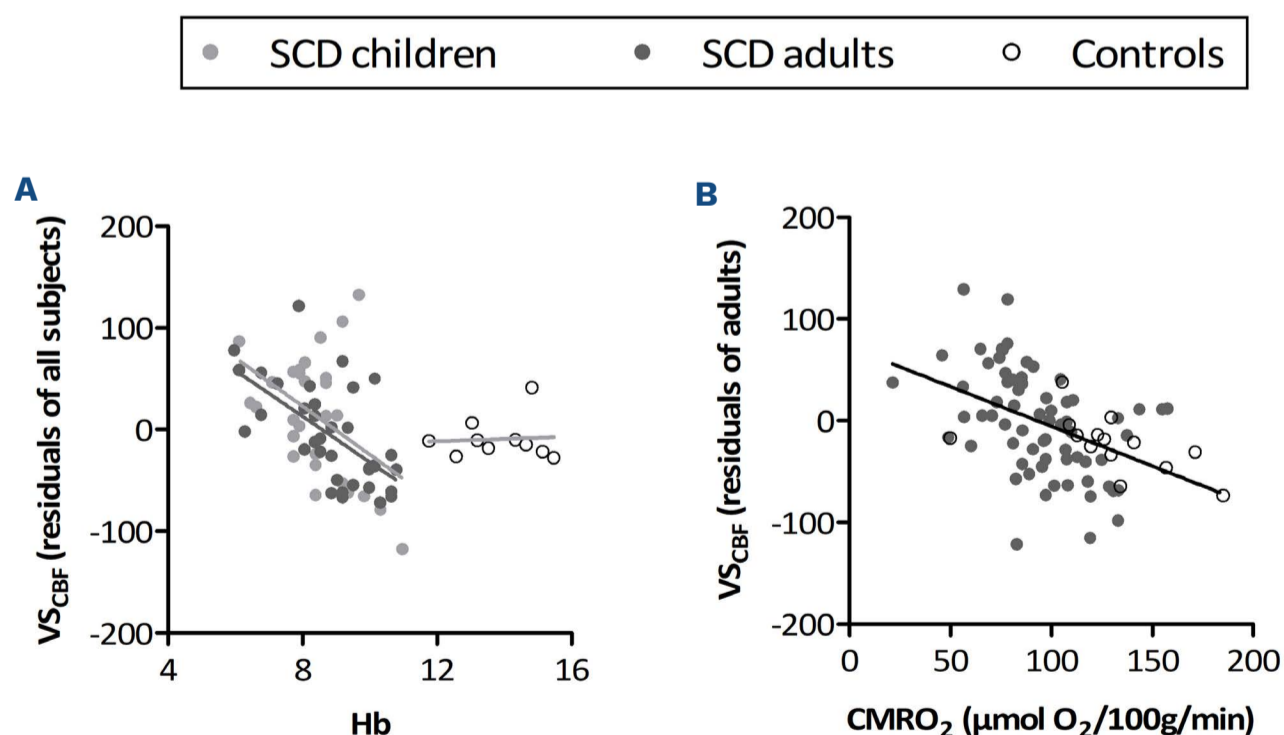


**Figure 5. Predictors of  $VS_{CBF}$**  Left: scatterplot of hemoglobin (Hb) and  $VS_{CBF}$  (the residual of the regression between venous signal [VS] and cerebral blood flow [CBF]) for all pre-acetazolamide (pre-ACZ) data of all subject groups. The association between Hb and  $VS_{CBF}$  was only significant in the patients, but not in controls. Right: scatterplot of cerebral metabolic rate of oxygen ( $CMRO_2$ ) and  $VS_{CBF}$  for the pre-ACZ and post-ACZ data in all adult subjects, showing a significant correlation across all subjects. Please note that the values for  $VS_{CBF}$  differ for both regressions as the pre-ACZ data were analyzed using multiple linear regression, whereas the pre-ACZ vs. post-ACZ data were analyzed using linear mixed models to accommodate the repeated measures variation.

another study demonstrated that, on multivariate analysis, LDH was the strongest predictor of DRBC, with bilirubin and HbF levels also retained in the model.<sup>42</sup>  $VS_{CBF}$  was comparable between pediatric and adult SCD patients, despite differences in absolute CBF. On the one hand, one might postulate higher  $VS_{CBF}$  in children because of their increased cerebral metabolic rates and greater risk for ischemic injury.<sup>43</sup> Alternatively, one might expect progressive microvascular damage and loss of cerebrovascular cross-sectional area with increasing age, similar to microvascular disease in other organs in SCD patients. A preliminary report assessing blood-brain barrier permeability demonstrated that children with SCD have higher PS than controls, despite lower extraction, suggesting increased functional capillary exchange area.<sup>44</sup> However, this remains to be confirmed in future studies that are encouraged to incorporate OEF and  $CMRO_2$  measurements from pediatric patients as well as age-matched healthy controls. This is important because SCI are also present in pediatric patients with SCD and it is, therefore, important to understand potential age-dependent underlying mechanisms.<sup>4,45</sup> We were unable to demonstrate any link between  $VS_{CBF}$  and white matter damage, however, the lesion load was relatively low, and no patients with overt stroke were included. Previous studies incorporating these samples also showed no association between lesion volume and

hemodynamic parameters.<sup>10,15</sup> Although evidence from neurodegenerative disorders and vascular disease suggest that there is a link between hypoxia and white matter lesions,<sup>46,47</sup> it remains to be determined how lower OEF and  $CMRO_2$ , and potentially functional shunting mechanisms are related to such lesions in patients with chronic anemia. A previous study<sup>20</sup> demonstrated a relationship between VS and OEF only in patients with a significant lesion load, but not in patients with overt stroke. However, they also did not correlate VS to lesion volumes. In this study,  $T_2$ -TRIR instead of TRUST was used to obtain venous oxygenation estimates for OEF calculation.  $T_2$ -TRIR enables  $T_1$  measurements in addition to  $T_2$  measurements. Given this advantage and a previous study showing OEF values in the same range as the values obtained from TRUST,<sup>22</sup> we opted for  $T_2$ -TRIR here. However, a recent study from our group<sup>48</sup> demonstrated that the OEF values obtained from  $T_2$ -TRIR were significantly lower compared to OEF values obtained from the TRUST sequence (despite comparable reproducibility), which may explain our lower OEF and  $CMRO_2$  values compared to previous studies using the TRUST sequence.<sup>20,33</sup> Additionally, we here used the HbS calibration model introduced by Bush et al.<sup>19</sup> to obtain the venous oxygenation in patients with SCD (although see the *Online Supplementary Appendix*, showing comparable findings using the HbA model for completeness). Recently, a novel sickle cell specific calibration

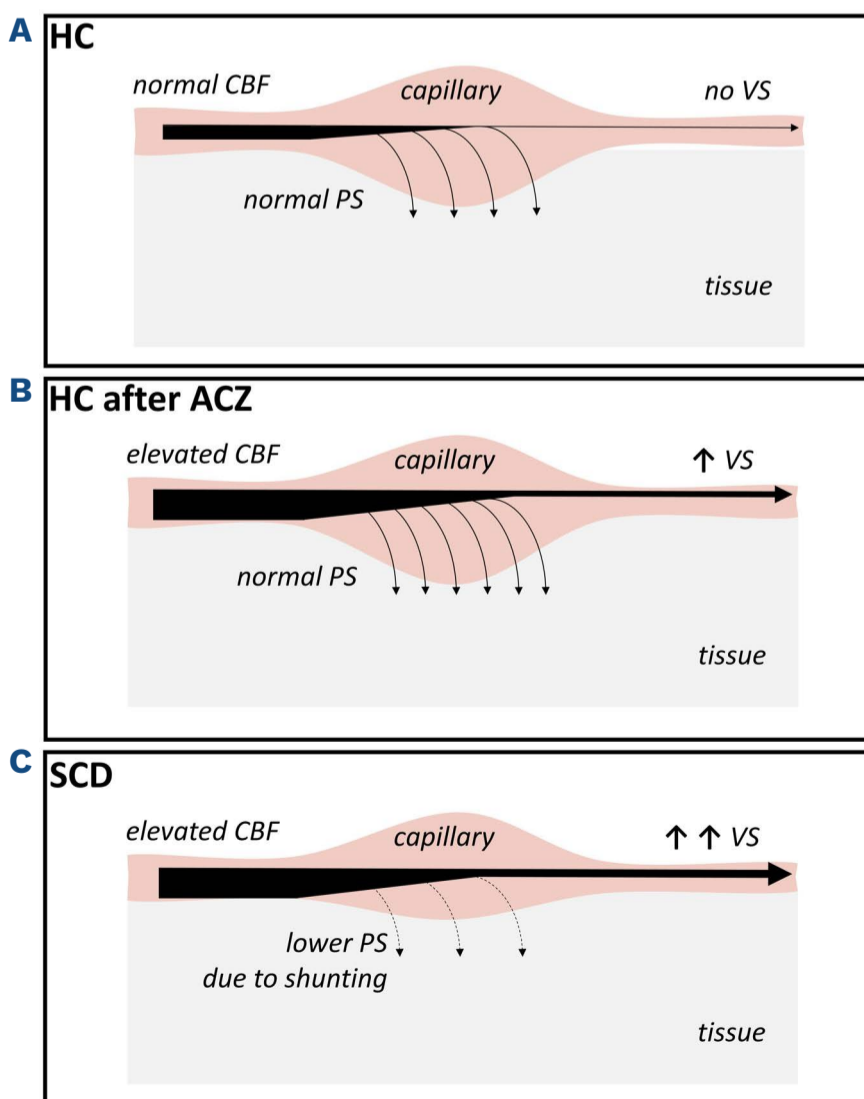


**Figure 6. Schematic hypothetical outline of venous signal in the absence and presence of shunting.** Arterially labeled spins enter brain parenchyma at a rate determined by the product of vascular surface area and intrinsic water permeability (permeability-surface area product). The re-entry of the label was previously shown to be negligible (Lin et al. 2018) and is therefore not displayed. (A) In the brain of a healthy control with normal cerebral blood flow (CBF) levels, (almost) no venous signal (VS) is observed. (B) In the brain of a healthy control after acetazolamide administration with increased CBF and intact permeability-surface area product (PS), VS signal can be observed as flow predominates the microvascular uptake. (C) In a patient with sickle cell disease (SCD) with the presence of shunting, blood preferentially passes through short, low resistance capillary pathways leading to functional loss of capillary surface area, further increasing VS and impairing oxygen unloading. HC: healthy control, ACZ: acetazolamide.

model, the Bush-Li model,<sup>49</sup> was introduced, based on a larger range of hematocrit. However, they did not show statistical superiority compared to the currently used Bush model, and therefore, we do not expect that our conclusions would be different using the Bush-Li model. An important strength of this study is the fact that we used a continuous estimate of VS, which allowed us to conduct regression analyses to investigate the relation between VS, hemodynamic measures and hematological parameters. However, our sample size is relatively small for multiple regression analyses, which is why we have carefully chosen our included predictors. Future studies should confirm our regression analyses using larger sample sizes, to further explore the presence of functional shunting and the associations between shunting and the parameters of oxygen metabolism. Furthermore, our pediatric sample did not include age-matched healthy controls. However, previous studies have already shown that CBF is higher in children with SCD compared to healthy children.<sup>9,15</sup> In addition, Wu et al.<sup>28</sup> showed that the signal in the sagittal sinus was lower in healthy children compared to children with SCD. Furthermore, the MRI scanner, the head coil and multiple scan parameters differed between the pediatric and adult patients, which precluded direct comparison of CBF and lesion volume estimates. Individual M0 scans were not acquired in our pediatric cohort, because the scanning was done prior to the M0 consensus recommendations in 2014.<sup>24</sup> Instead, we used a single fixed M0 value to quantify CBF. In a *post hoc* analysis in adults, we found comparable coefficients of variation for GM CBF obtained from a group average M0 and from a subject-specific M0. Moreover, using a group average M0 did not change the associations between VS and the parameter GM CBF and the markers Hb and LDH. Nevertheless, using a single M0 value does not account for slight spatial differences in magnetization, which is why a subject-specific M0 was used in our adult participants and why this is also recommended for future studies. Additionally, the T<sub>2</sub>-TRIR scan was not available for the pediatric study, and therefore OEF and CMRO<sub>2</sub> estimates could not be obtained in pediatric patients. In the adults, only a small proportion of patients were on chronic exchange transfusion, and therefore its effect could not be estimated in this study. Although hydroxyurea did not appear to affect the relationships found in this study, future studies in larger samples could shed

light on the effects of hydroxyurea treatment on functional shunting. Our control group included two sickle cell trait participants whose hematological parameters and T<sub>2</sub> values were in the same range as those of the HbAA controls, in line with previous studies.<sup>19,50</sup> This suggests that they were appropriately included as control subjects.

In summary, our findings suggest that higher CBF-corrected venous signal may reflect the loss of capillary exchange area as shown by its relationship to CMRO<sub>2</sub>, providing evidence for cerebral functional shunting. Moreover, we found that higher disease severity is related to higher VS and that CMRO<sub>2</sub> is additionally influenced by HbF and LDH. These findings indicate that the venous signal on ASL images can be considered as a complementary biomarker of cerebral perfusion and oxygen metabolism.

### Disclosures

BB has financial relationship with GBT, Novartis, Sanquin, Novo nordisk, Celgene, CSL Behring, CHIESI and Bluebird Bio. LV has a financial relationship with Philips Healthcare.

### Contributions

LAH was involved in the study conception and design, analysis and interpretation of the data and manuscript drafting; LV and BJB were involved in data acquisition, analysis and interpretation of the data and manuscript revision; JCW was involved in analysis and interpretation of the data and manuscript revision; AJN and HJMMM were involved in study conception and design, analysis and interpretation of the data and manuscript revision; AS was involved in analysis and interpretation of the data and manuscript drafting..

### Acknowledgements

The authors would like to thank all the participants for their time and effort to take part in this study and they are grateful to Dr. Jan Petr for his advice regarding ExploreASL.

### Funding

The authors disclose receipt of the following financial support for the research, authorship, and/or publication of this article: National Heart Lung and Blood Institute (1R01HL136484-A1).

### Data-sharing statement

Data available on request from the authors.

## References

1. Rees DC, Williams TN, Gladwin MT. Sickle-cell disease. *Lancet*. 2010;376(9757):2018-2031.
2. Debaun MR, Kirkham FJ. Central nervous system complications and management in sickle cell disease. *Blood*. 2016;127(7):829-838.
3. Strouse JJ, Jordan LC, Lanzkron S, et al. The excess burden of stroke in hospitalized adults with sickle cell disease. *Am J Hematol*. 2009;84(9):548-552.
4. Ford AL, Ragan DK, Fella S, et al. Silent infarcts in sickle cell disease occur in the border zone region and are associated

- with low cerebral blood flow. *Blood*. 2018;132(16):1714-1723.
5. Bernaudin F, Verlhac S, Arnaud C, et al. Chronic acute anemia and extracranial internal carotid stenosis are risk factors for silent cerebral infarcts in sickle cell anemia. *Blood*. 2015;125(10):1653-1661.
  6. van der Land V, Mutsaerts HJMM, Engelen M, et al. Risk factor analysis of cerebral white matter hyperintensities in children with sickle cell disease. *Br J Haematol*. 2016;172(2):274-284.
  7. Herold S, Brozovic M, Gibbs J, et al. Measurement of regional cerebral blood flow, blood volume and oxygen metabolism in patients with sickle cell disease using positron emission tomography. *Stroke*. 1986;17(4):692-698.
  8. Numaguchi Y, Haller JS, Humbert JR, et al. Cerebral blood flow mapping using stable Xenon-enhanced CT in sickle cell cerebrovascular disease. *Neuroradiology*. 1990;32(4):289-295.
  9. Oguz KK, Golay X, Pizzini FB, et al. Sickle cell disease: continuous arterial spin-labeling perfusion MR imaging in children. *Radiology*. 2003;227(2):567-574.
  10. Václavů L, Petr J, Petersen ET, et al. Cerebral oxygen metabolism in adults with sickle cell disease. *Am J Hematol*. 2020;95(4):401-412.
  11. Kassim AA, Pruthi S, Day M, et al. Silent cerebral infarcts and cerebral aneurysms are prevalent in adults with sickle cell anemia. *Blood*. 2016;127(16):2038-2040.
  12. Bush A, Chai Y, Choi SY, et al. Pseudo continuous arterial spin labeling quantification in anemic subjects with hyperemic cerebral blood flow. *Magn Reson Imaging*. 2018;47:137-146.
  13. Juttukonda MR, Donahue MJ, Davis LT, et al. Preliminary evidence for cerebral capillary shunting in adults with sickle cell anemia. *J Cereb Blood Flow Metab*. 2019;39(6):1099-1110.
  14. Van Den Tweel XW, Nederveen AJ, Majoie CBLM, et al. Cerebral blood flow measurement in children with sickle cell disease using continuous arterial spin labeling at 3.0-tesla MRI. *Stroke*. 2009;40(3):795-800.
  15. Gevers S, Nederveen AJ, Fijnvandraat K, et al. Arterial spin labeling measurement of cerebral perfusion in children with sickle cell disease. *J Magn Reson Imaging*. 2012;35(4):779-787.
  16. Lin Z, Li Y, Su P, et al. Non-contrast MR imaging of blood-brain barrier permeability to water. *Magn Reson Med*. 2018;80(4):1507-1520.
  17. Renkin EM. Transport of potassium-42 from blood to tissue in isolated mammalian skeletal muscles. *Am J Physiol*. 1959;197:1205-1210.
  18. Crone C. The permeability of capillaries in various organs as determined by use of the 'indicator diffusion' method. *Acta Physiol Scand*. 1963;58:292-305.
  19. Bush AM, Coates TD, Wood JC. Diminished cerebral oxygen extraction and metabolic rate in sickle cell disease using T2 relaxation under spin tagging MRI. *Magn Reson Med*. 2018;80(1):294-303.
  20. Juttukonda MR, Donahue MJ, Waddle SL, et al. Reduced oxygen extraction efficiency in sickle cell anemia patients with evidence of cerebral capillary shunting. *J Cereb Blood Flow Metab*. 2020;41(3):546-560.
  21. Václavů L, Meynart BN, Mutsaerts HJMM, et al. Hemodynamic provocation with acetazolamide shows impaired cerebrovascular reserve in adults with sickle cell disease. *Haematologica*. 2019;104(4):690-699.
  22. De Vis JB, Petersen ET, Alderliesten T, et al. Non-invasive MRI measurements of venous oxygenation, oxygen extraction fraction and oxygen consumption in neonates. *Neuroimage*. 2014;95:185-192.
  23. Vaclavu L, Van Der Land V, Heijtel DFR, et al. In vivo T1 of blood measurements in children with sickle cell disease improve cerebral blood flow quantification from arterial spin-labeling MRI. *Am J Neuroradiol*. 2016;37(9):1727-1732.
  24. Alsop DC, Detre JA, Golay X, et al. Recommended implementation of arterial spin-labeled perfusion MRI for clinical applications: a consensus of the ISMRM Perfusion Study group and the European consortium for ASL in dementia. *Magn Reson Med*. 2015;73(1):102-116.
  25. Zhao MY, Václavů L, Petersen ET, et al. Quantification of cerebral perfusion and cerebrovascular reserve using Turbo-QUASAR arterial spin labeling MRI. *Magn Reson Med*. 2020;83(2):731-748.
  26. Mutsaerts H, Petr J, Groot P, et al. ExploreASL: an image processing pipeline for multi-center ASL perfusion MRI studies. *Neuroimage*. 2020;219:117031.
  27. Evans AC, Janke AL, Collins DL, et al. Brain templates and atlases. *Neuroimage*. 2012;62(2):911-922.
  28. Wu WC, St Lawrence KS, Licht DJ, et al. Quantification issues in arterial spin labeling perfusion magnetic resonance imaging. *Top Magn Reson Imaging*. 2010;21(2):65-73.
  29. Stotesbury H, Hales PW, Koelbel M, et al. Venous cerebral blood flow quantification and cognition in patients with sickle cell anemia. *J Cereb Blood Flow Metab*. 2022;42(6):1061-1077.
  30. Jespersen SN, Østergaard L. The roles of cerebral blood flow, capillary transit time heterogeneity, and oxygen tension in brain oxygenation and metabolism. *J Cereb Blood Flow Metab*. 2012;32(2):264-277.
  31. Sakadžić S, Mandeville ET, Gagnon L, et al. Large arteriolar component of oxygen delivery implies a safe margin of oxygen supply to cerebral tissue. *Nat Commun*. 2014;5:5734.
  32. Jordan LC, Gindville MC, Scott AO, et al. Non-invasive imaging of oxygen extraction fraction in adults with sickle cell anaemia. *Brain*. 2016;139(Pt 3):738-750.
  33. Vu C, Bush A, Choi S, et al. Reduced global cerebral oxygen metabolic rate in sickle cell disease and chronic anemias. *Am J Hematol*. 2021;96(8):901-913.
  34. Williams KP, Fields ME, Ragan DK, et al. Red cell exchange transfusions lower cerebral blood flow and oxygen extraction fraction in pediatric sickle cell anemia. *Blood*. 2018;131(9):1012-1021.
  35. Croal PL, Leung J, Phillips CL, et al. Quantification of pathophysiological alterations in venous oxygen saturation: A comparison of global MR susceptometry techniques. *Magn Reson Imaging*. 2019;58:18-23.
  36. Wang Y, Fella S, Fields ME, et al. Cerebral oxygen metabolic stress, microstructural injury, and infarction in adults with sickle cell disease. *Neurology*. 2021;97(9):e902-e912.
  37. Hambley BC, Rahman RA, Reback M, et al. Intracardiac or intrapulmonary shunts were present in at least 35% of adults with homozygous sickle cell disease followed in an outpatient clinic. *Haematologica*. 2019;104(1):e1-e3.
  38. Dowling MM, Quinn CT, Ramaciotti C, et al. Increased prevalence of potential right-to-left shunting in children with sickle cell anaemia and stroke. *Br J Haematol*. 2017;176(2):300-308.
  39. DeBeer T, Jordan LC, Lee CA, et al. Evidence of transfusion-induced reductions in cerebral capillary shunting in sickle cell disease. *Am J Hematol*. 2020;95(9):E228-E230.
  40. Young RC, Rachal RE, Del Pilar Aguinaga M, et al. Automated oxyhemoglobin dissociation curve construction to assess sickle cell anemia therapy. *J Natl Med Assoc*. 2000;92(9):430-435.
  41. Di Liberto G, Kiger L, Marden MC, et al. Dense red blood cell and oxygen desaturation in sickle-cell disease. *Am J Hematol*. 2016;91(10):1008-1013.
  42. Bartolucci P, Brugnara C, Teixeira-Pinto A, et al. Erythrocyte density in sickle cell syndromes is associated with specific

- clinical manifestations and hemolysis. *Blood*. 2012;120(15):3136-3141.
43. DeBaun MR, Sarnaik SA, Rodeghier MJ, et al. Associated risk factors for silent cerebral infarcts in sickle cell anemia: Low baseline hemoglobin, sex, and relative high systolic blood pressure. *Blood*. 2012;119(16):3684-3690.
44. Lin Z, Lance E, Li Y, et al. Impaired blood-brain barrier function in pediatric sickle cell disease. In: ISMRM 27th Annual Meeting & Exhibition, Montreal, Canada, 11-16 May 2019, Abstract #0738
45. DeBaun MR, Armstrong FD, McKinstry RC, et al. Silent cerebral infarcts: a review on a prevalent and progressive cause of neurologic injury in sickle cell anemia. *Blood*. 2012;119(20):4587-4596.
46. Yatawara C, Lee D, Ng KP, et al. Mechanisms linking white matter lesions, tract integrity, and depression in alzheimer disease. *Am J Geriatr Psychiatry*. 2019;27(9):948-959.
47. Van Dijk EJ, Prins ND, Vrooman HA, et al. Progression of cerebral small vessel disease in relation to risk factors and cognitive consequences: Rotterdam scan study. *Stroke*. 2008;39(10):2712-2719.
48. Baas K, Coolen B, Petersen E, et al. Comparative analysis of blood T2 values measured by T2-TRIR and TRUST. *J Magn Reson Imaging*. 2022;56(2):516-526.
49. Bush A, Vu C, Choi S, et al. Calibration of T2 oximetry MRI for subjects with sickle cell disease. *Magn Reson Med*. 2021;86(2):1019-1028.
50. Eaton W, Hofrichter J. Hemoglobin S gelation and sickle cell disease. *Blood*. 1987;70(5):1245-1266.